Pergamon

Progress in Oceanography 47 (2000) 337–354

Progress in Oceanography

www.elsevier.com/locate/pocean

Chaos in the North Pacific: spatial modes and temporal irregularity

J.E. Overland [a,*], J.M. Adams [b], H.O. Mofjeld [a]

[a] *Pacific Marine Environmental Laboratory/NOAA, 7600 Sand Point Way N.E., Seattle, WA 98115-6349, USA*

[b] *JISAO/University of Washington, Box 351640, Seattle, WA 98195, USA*

Abstract

The small amount of North Pacific SST variance explained by the first two organized modes, as well as the irregular nature of the decadal-interdecadal variability of SSTs and spatial atmospheric forcing, suggest that a low order, nonlinear, chaotic system of atmospheric/oceanic variability may be acting in the North Pacific. Systems, which visit many states yet tend to return to the vicinity of previously observed patterns, have properties similar to mathematical chaos. Wavelet analyses of the wintertime Pacific Decadal Oscillation, Aleutian Low intensity from 1900, and Sitka air temperatures from 1832 suggest broad-banded time series with irregular oscillatory behavior. The different frequency bands do not appear to be independent; their alignment has resulted in major shifts around 1847, 1880?, 1925, 1945, 1977, and minor shifts in 1958 and 1989. Although the observational time series are too short to prove that the coupled atmosphere and ocean in the North Pacific is chaotic, the notion that it is stable for decadal periods and then exhibits rapid transitions is the basis for our conceptual model. This model suggests that the North Pacific system is less sensitive to external forcing when it is near one of its stable states. At other times the system is more responsive to short-term extreme events such as ENSO, Siberian snow cover, hemispheric atmospheric modes, or local SST anomalies. Increased interannual variability is expected around the times of interdecadal shifts. Recent persistence of La Niña as well as enhanced interannual variability in several other time series, are consistent with a possible shift of the PDO in 1999. © 2000 Published by Elsevier Science Ltd.

* Corresponding author. Tel.: +1(206)526-6795; fax: +1(206)526-6485.
E-mail address: overland@pmel.noaa.gov (J.E. Overland).

0079-6611/00/$ - see front matter
PII: S0079-6611(00)00041-0

Contents

1. Introduction 338

2. Data sources 340

3. Spatial patterns 340

4. Time-frequency analysis 343

5. Chaos in the North Pacific 347
5.1. Irregular variability in the North Pacific 347
5.2. Characteristics of chaotic systems 348
5.3. A chaotic conceptual model for the North Pacific 350

6. Summary 352

Acknowledgements 352

References 353

1. Introduction

In building a conceptual model of climate dynamics for the North Pacific atmosphere and ocean, it is important to consider not only the fixed geographic patterns of variability, but also the range and evolution of the system. The primary mode of SST variability in the North Pacific is called the Pacific Decadal Oscillation (PDO) (Davis, 1976; Mantua, Hare, Zhang, Wallace & Francis, 1997). The PDO explains about 20% of the wintertime (November–March) SST variance based on empirical orthogonal function (EOF) analysis. The spatial pattern of the PDO is dominated by the central North Pacific with a maximum intensity at 40°N, 170°W (Fig. 1); the principal component time series (Fig. 1) is dominated by variability on pentadecadal (~50 year) scales. A problem with the definition of the PDO is that the spatial correlation length for the SST field is nearly equivalent to the size of the Pacific basin; this overweights the variability in the center of the region relative to the borders. In order to understand the biological and physical processes in the boundary regions, the variability in these important domains must be carefully and correctly resolved.

The relatively small percentage of variance explained by the PDO indicates that it is not the only mode of variability in the Northeast Pacific. Variability on shorter time scales has been observed in ocean temperatures (Royer, 1993; Hollowed, Hare & Wooster, 1998), dynamic height (Lagerloef, 1995), and in the Aleutian low sea level pressure (SLP) center (Minobe, 1999; Overland, Adams & Bond, 1999). The month-to-month and year-to-year variability in the strength and location of the Aleutian low influences the underlying ocean (Seckel, 1993). One purpose of this

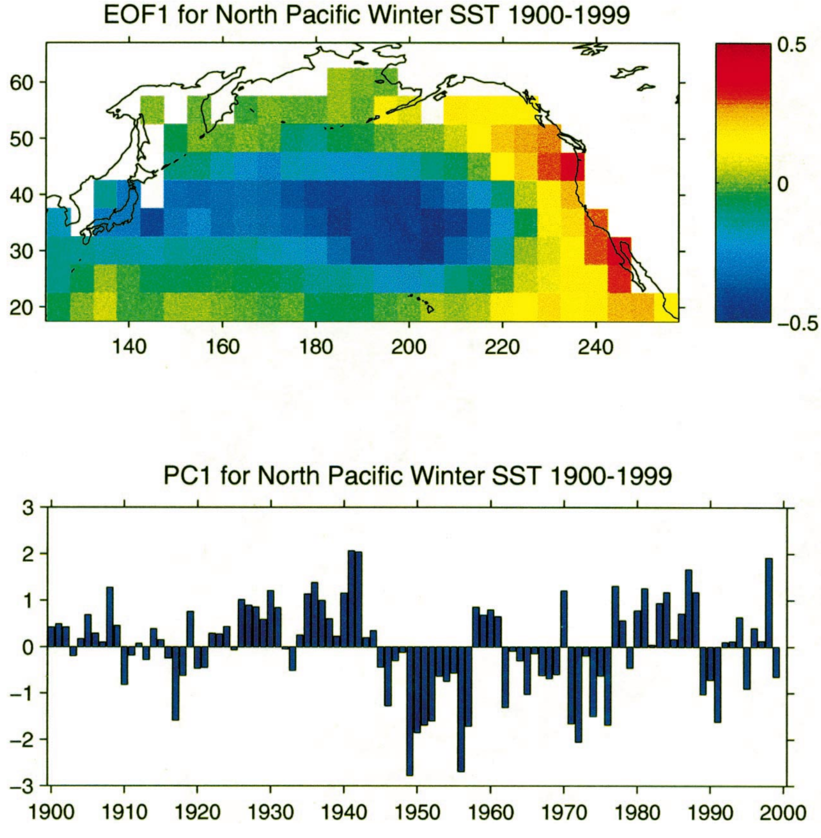

Fig. 1. Results of the singular value decomposition of the winter mean (November–Mar) North Pacific SST for the period 1900–1999. Top panel shows the first EOF and the bottom panel shows its principal component (PC) time series. This primary mode of variability is called the Pacific Decadal Oscillation.

paper then is to examine the residual variability in the North Pacific after the PDO has been removed. We refer to this as Mode 2 variability.

A second purpose is to use wavelets to investigate how the North Pacific varies in the time-frequency domain. We compare the SST and SLP time series to the record of surface air temperature at Sitka, Alaska, which dates back to 1828. The Sitka data are used as a proxy for North Pacific variability in the 19th century.

We propose that the behavior of the North Pacific atmosphere and ocean have several characteristics of a chaotic system. We do not use the word chaos in the general sense to denote disorder, but rather in a mathematical context to indicate complex nonperiodic behavior in a deterministic system. The North Pacific maps out an infinite variety of states within certain bounds which determine its climate. Chaos is often described as the divergence of two states, but chaotic systems do return to the vicinity of previously observed states. This gives the appearance of quasi-regular modes of variability without being strictly periodic.

Section 2 discusses the data sources used in our analyses. Section 3 describes several approaches to defining Mode 2 spatial variability. Section 4 contains an analysis of atmospheric and oceanic time-frequency variability using wavelet techniques. Section 5 compares several characteristics of the North Pacific to simple chaotic systems. The summary appears in Section 6.

2. Data sources

Monthly SST anomalies on a 5° lat/lon grid are from the UK Meteorological Office Sea Surface Temperature Data Set, which is based only on in situ data (Parker, Folland & Jackson, 1995). Our EOF analyses follows the technique used by Mantua et al. (1997) to calculate the PDO. However, our results differ slightly from theirs because we use the UKMET data exclusively. The spatial domain is restricted to 172 grid points in the North Pacific between 20°N–65°N and 120°E–105°W. The time domain is November 1899 through March 1999. First, a monthly time series of global average SST anomalies is calculated using all available data between 35°S–70°N; this shows a distinct global warming trend for the 20th century. This trend is removed by subtracting the monthly global average anomaly from each available grid point in the North Pacific. Grid points with missing data in the detrended North Pacific SST anomaly data set are filled with the mean calculated from all available data at that grid point. Then the overall mean of the patched, detrended North Pacific SST anomaly data set is removed, so that the grid points that were originally missing have a value of zero.

The North Pacific Index (NPI), as defined by Trenberth and Hurrell (1994), is the area weighted mean sea level pressure over the region 30°–65°N, 160°E–140°W. We use the NCAR 5-degree Northern Hemisphere monthly sea level pressure data set to calculate the NPI. The Sitka Alaska time series of monthly mean surface air temperature was provided by Tom Royer.

3. Spatial patterns

Fig. 1 shows the first EOF and principal component (PC) time series for winter average (November–March) North Pacific SST data, 1899–1999. EOF1 accounts for 21% of the variance. EOF1 is not regressed back onto the SST field as it was in Mantua et al. (1997). Nearly the same spatial pattern and principal components were obtained for EOF1 if we performed the analysis on the time series beginning in 1950 (Fig. 3). Some regions are missing data, especially in the early part of the century, so we checked individual grid points in the North Pacific to ensure that the time series of SST observations actually warrants an analysis of low frequency variability. The central region of the North Pacific, which dominates EOF1, is adequately covered by the North America/Asia shipping route.

The second EOF of North Pacific SST for 1950–1999 is shown in Fig. 2 and the PC time series is shown in Fig. 3. EOF2 was not consistent when analyzing the

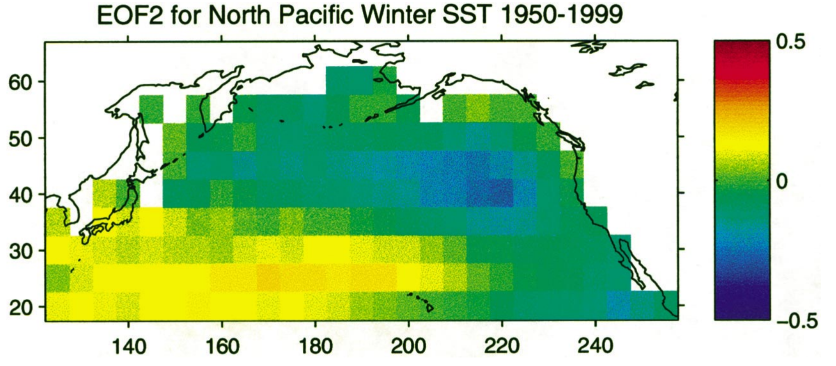

Fig. 2. The second EOF based on the singular value decomposition of the winter mean (November–March) North Pacific SST for the period 1950–1999.

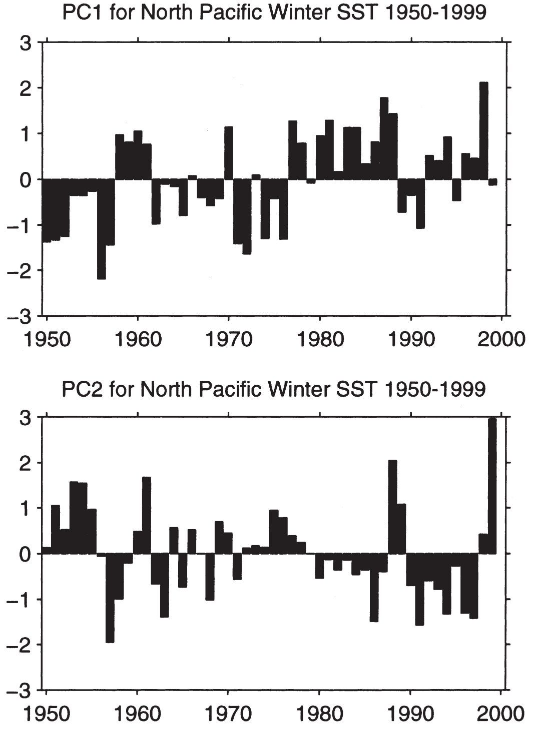

Fig. 3. Principal component time series for EOF1 and EOF2 based on the singular value decomposition of winter mean (November–March) North Pacific SST for the period 1950–1999.

1900–1999 data set versus the 1950–1999 data set. In using the entire 1900–1999 data set there was considerable amplitude in the Kuroshio region that is not present in Fig. 2. The paucity of data in the Gulf of Alaska prior to 1950 also lead us to use the shortened series to investigate the secondary mode of North Pacific SST variability. For the period 1950–1999, EOF1 accounts for 29.1% of the variance and EOF2 accounts for 13.1% of the variance. These two modes are nearly identical to the EOFs derived by Davis (1976) and Salmon (1992).

The spatial pattern and PC time series for EOF2 have a different character from those of EOF1 (Fig. 3). EOF2 has more of zonal character than EOF1; PC1 tends to have serially correlated amplitudes, while PC2 tends to have strong interannual spikes. These spikes occur near the onset of several but not all occurrences of El Niño (1957, 1958, 1963, 1986, 1991, 1997) and La Niña (1953, 1954, 1961, 1988, 1999). The peaks in PC2 tend to occur in the year before the major El Niño/La Niña signal appears in the central and eastern equatorial Pacific. Perhaps PC2 is responsive to the ENSO build-up in the western equatorial Pacific. The relationship between North Pacific SSTs and ENSO has been referred to as Niño North (Hollowed et al., 1998). During some ENSOs enhanced midlatitude storm activity weakens the Niño North signature (Hoerling & Kumar, 1997); the strong ENSO of 1983 is such an example and contrasts to the weaker ENSOs of 1958 and 1987, which do have a substantial Niño North signal.

Cluster analysis and point-to-point correlations offer an alternative to EOF analysis for understanding patterns of spatial variability. A cluster analysis for winter North Pacific SST based on 1969–1979 is shown in Fig. 4 (Iwasaka, Hanawa & Toba, 1988). The cluster analysis separates the central North Pacific (region C) and the boundary (region D) by minimizing the point-to-point variance within each area. Based on SST data for 1953–1990, Salmon (1992) noted that the correlation of EOF1 with Iwasaka's central region C was 0.90, but with the boundary region D it was −0.51. For EOF2 the correlation with the central region C was 0.30 and the boundary

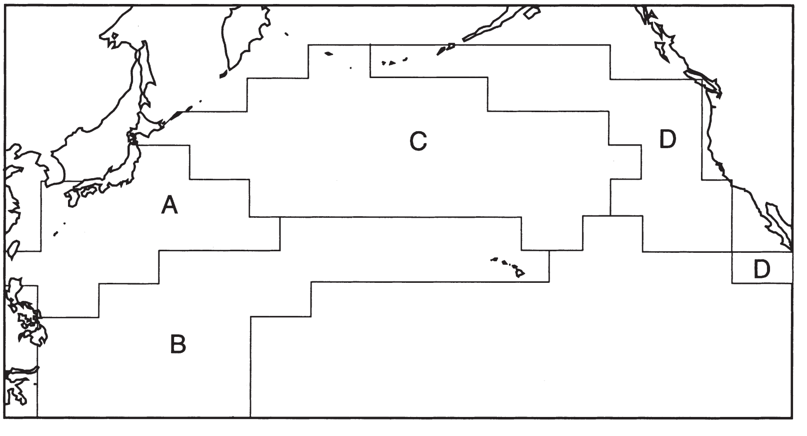

Fig. 4. Results of cluster analysis for the North Pacific SST (after Iwasaka et al., 1988).

region D was 0.82. This suggests that the SST variability in the northeast Pacific region dominates Mode 2, while the central Pacific dominates the PDO.

To describe the Mode 2 variability further, we subtracted the regression of the wintertime PDO of Mantua et al. (1997) from the time series of North Pacific SST and performed a point-to-point correlation between a grid cell in the northeast Pacific (57°N, 148°W) and the field of resulting SSTs. The results are shown in Fig. 5. There is a broad region of high correlation: south of the Aleutian Islands, across the Gulf of Alaska, and southeast past Vancouver Island. Mode 2 appears to be particularly relevant for the Gulf of Alaska region.

There are differences between the Mode 2 figures created by EOF analysis (Fig. 2), cluster analysis (Fig. 4), and point-to-point correlation (Fig. 5). The cluster analysis emphasizes a broad coastal influence from Mexico northward and across the Aleutian Island chain. The EOF2 analysis is a NNE/SSW dipole with the northeast Pacific out of phase with the west North Pacific centered near 25°N and may not resolve the coastal region. The point-to-point correlation shows strong zonal covariability. All three approaches suggest that the Northeast Pacific is dominant in Mode 2, but no single approach is complete in specifying a spatial pattern.

About 40% of the North Pacific winter SST variability on interannual and longer timescales is represented by the combination of the PDO and Mode 2. Winter mean SST anomalies for individual years exhibit a PDO character in the late 1950s and early 1980s and a more zonal pattern in the 1960s and early 1990s, but much of the spatial variability remains unresolved by these patterns. The North Pacific exhibits a few preferred modes of variability, but the system is energetic and can manifest many states.

4. Time-frequency analysis

We performed a continuous wavelet analysis on winter average values (November–March) of the PDO. We used the PDO index values of Mantua et al.

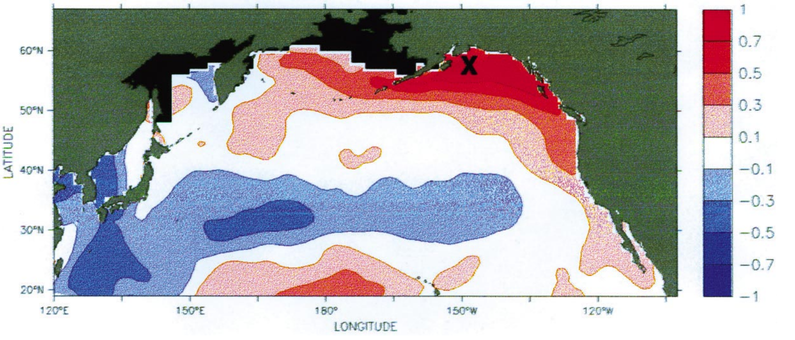

Fig. 5. Results of a point-point correlation analysis for the residual SST, i.e., that which remains after the regression of the PDO on the winter mean SST has been removed. Correlations are between a grid cell in the Gulf of Alaska (57°N, 148°W; marked with an ×) and the rest of the North Pacific for the period 1962–1997. Grid cells with insufficient data are blacked out.

(1997) rather than our own PC1 time series to be consistent with the community definition of the PDO. We used the symlet transform, order 8, from the MATLAB software (Daubechies, 1994). We also applied the Morlet wavelet transform with similar results. See Lau and Weng (1995) and Torrence and Campo (1998) for a review of wavelets.

The results of the continuous wavelet analysis of the PDO are shown in the bottom panel of Fig. 6 with the year on the abscissa and the return period (years) on the ordinate. It is apparent from a casual inspection of the time series (Fig. 6, top) and the wavelet analysis that there is considerable energy in the low frequencies (16–32 years) and a less coherent signal at higher frequencies (2–8 years). We also note an increase in the mid-range energy (8–16 years) after 1940.

Fig. 7 shows the time series and wavelet analysis for the NPI, an index of the strength of the Aleutian low, which is the primary atmospheric forcing for the PDO. The results are nearly identical to those of Minobe (1999), who used the Morlet wavelet transform. The patterns of time–frequency variability in the NPI and the PDO are generally similar with only a few differences. The low frequency cycles

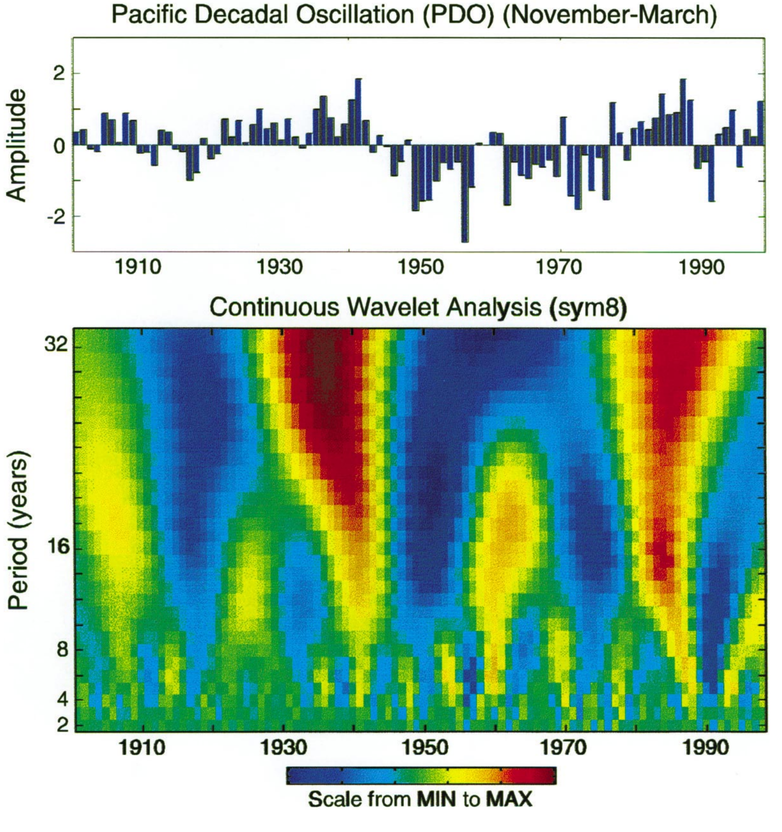

Fig. 6. Top panel shows the time series of winter mean PDO amplitudes as calculated by Mantua et al. (1997) for 1901–1999. The bottom panel shows the results of the continuous wavelet analysis.

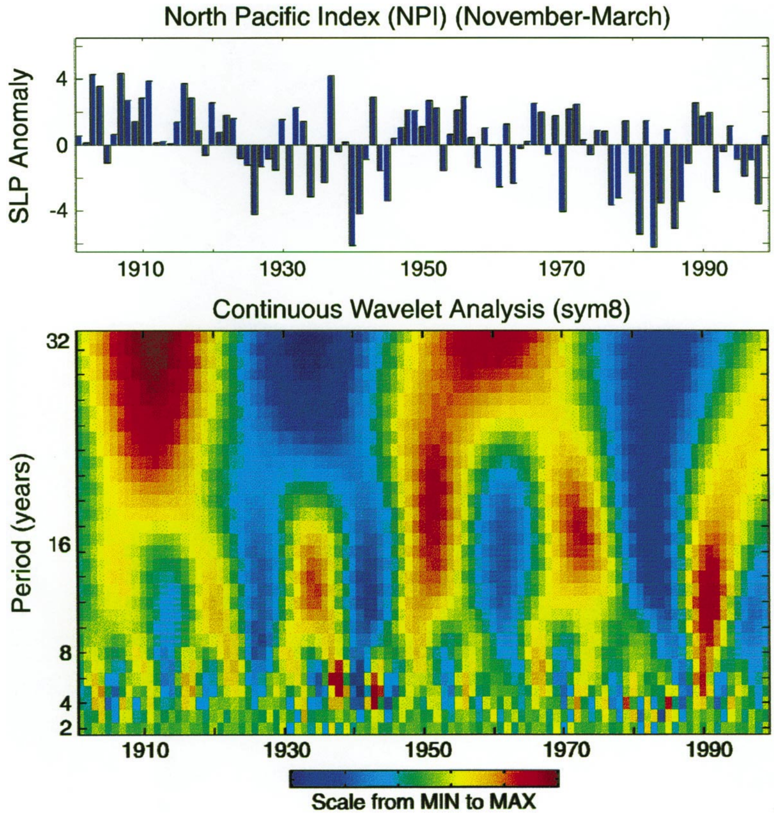

Fig. 7. Top panel shows the time series of winter mean North Pacific SLP Index (NPI) for 1901–1999. The bottom panel shows the results of the continuous wavelet analysis.

in the NPI and the PDO are nearly identical. The signal in the mid-range is stronger in the NPI than the PDO, but the phasing is nearly identical. Like the PDO, the mid-range energy of the NPI appears to increase toward the second half of the century. Minobe (1999) noted the mid-range energy maxima in the NPI shifted in 1945 from 8-year periods to 16-year periods. The NPI has more energy than the PDO at higher frequencies — this is also evident in the NPI time series, which shows considerable interannual variability. The PDO appears responsive to the interdecadal (~20 year cycle) forcing from the North Pacific atmosphere in the second half of the century, but is not particularly responsive to decadal and interannual atmospheric signals.

Coastal air temperature at Sitka, Alaska, is the longest observational record available for the Gulf of Alaska (Royer, 1993). The time series spans the years 1828–1996 with some data gaps before 1900, most noticeably in the 1890s; note the flat places in the time series (Fig. 8, top). The continuous wavelet analysis of the Sitka air temperature (SAT) is shown in the bottom panel of Fig. 8. The low frequency variability in the 20th century is similar in phase to the NPI and PDO. In the 19th

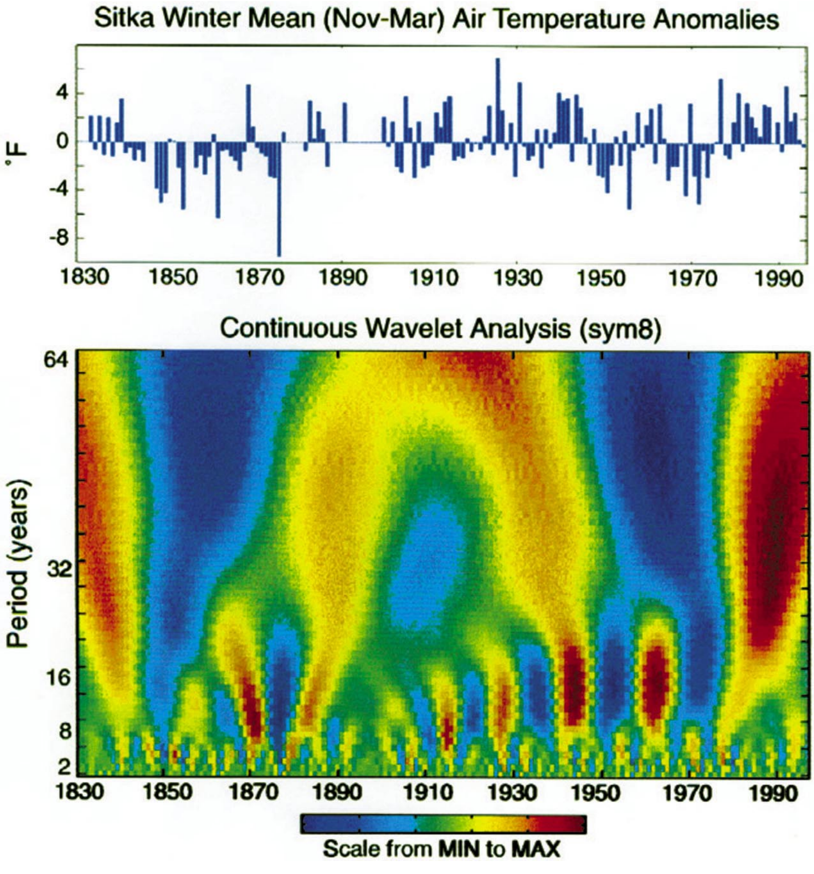

Fig. 8. Top panel shows the time series of winter mean air temperatures in Sitka, Alaska for 1829–1996. Note some missing data between 1880 and 1900. The bottom panel shows the results of the continuous wavelet analysis.

century there is a low frequency shift near 1847 and possibly a warm period beginning near 1880, although this is near the data gaps. The mid-range energy is particularly strong from 1940–1980. Royer (1989) noted that beginning in 1910 the warm/cold cycles increased in duration as the century progressed, resulting in zero crossings after 9, 13, 19, and 23 years. This progression is seen clearly in the wavelet analysis. The data gaps influence the analysis for a 16-year period near the turn of the century, but they do not influence the mid-range cycles after 1910. The Sitka record shows primarily decadal variability in the period from 1860–1890 and an increase in the mid-range energy in the second half of the 20th century. As noted above, similar mid-range energy shifts around 1945 also appeared in the PDO and the NPI.

Minobe (1999) discusses a possible resonance in interdecadal and pentadecadal climate oscillations in the North Pacific. Bidecadal oscillations have one and a half cycles for each half cycle of the pentadecadal. The phases for the interdecadal and pentadecadal variations are additive, resulting in large climate regime shifts in 1945 and 1977. Our wavelet analyses suggests that the interdecadal oscillations have been stronger in the second half of the 20th century. There is also evidence for smaller decadal shifts in 1958 (Leathers & Palecki, 1992) and 1989 (Tanaka, Kanohgi & Yasunari, 1996; Overland et al., 1999; Watanabe & Nitta, 1999).

A discrete (as opposed to the continuous) wavelet analysis is performed on the winter average time series as an appropriate method for quantitatively investigating broad-banded, low-frequency variability (Percival & Mofjeld, 1997). This approach acts as an efficient frequency filter. Table 1 shows the percent variance from each frequency band. The main feature seen from Table 1 is the broad banded nature of all three time series. For the NPI and Sitka time series interannual variability (2–4 years) dominates with nearly 40% of the variance. Next in importance for all three series is the 4–8-year band, considered to have an El Niño influence. The PDO has a local minimum at the decadal scale (8–16 years) and 27% of the variance is a time scale longer than 32 years. There is variance in the interdecadal band (16–32 years), which is concentrated in the second half of the century (Fig. 6). Both the Aleutian low (NPI) and the Sitka air temperatures have representation in all lower frequency bands beginning at the decadal scale. However, inspection of the continuous wavelets (Figs. 7 and 8) show that the time series are not stationary; the relative importance of different frequency bands shifts with time.

5. Chaos in the North Pacific

5.1. Irregular variability in the North Pacific

There are several features of the low frequency variability of the North Pacific that are worth noting:

1. About 40% of the North Pacific SST variability on interannual and longer time-scales is resolved by the first two spatial modes.
2. The energy of the PDO in the interdecadal band increased in the second half of the century relative to the first half.

Table 1
Fractional variance for each wavelet band for three time series

Years	PDO (%)	NPI (%)	Sitka air temperature (%)
2–4	25.8	39.2	40.9
4–8	19.2	27.4	21.4
8–16	11.0	10.4	13.6
16–32	16.1	8.7	9.3
32–64	14.9	11.6	7.0
64+	12.0	2.5	7.8

3. There is a drift in the oscillation periods in the decadal and interdecadal energy bands. The PDO has a zero crossing time of ~20 years before 1945 and ~30 after 1945. The cycle periods of the NPI and Sitka air temperatures gradually increase throughout the 20th century.
4. The interdecadal energy band seems to be phase locked with the pentadecadal band. This process is called doubling. Minobe (1999) states that this phase lock is not likely to occur from random superposition of two frequencies.
5. The low-frequency variability is near the frequencies of natural forcing: 11 and 22 years for the solar cycle and 18.6 years for the lunar cycle, although the strength of the forcing is weak (Lean & Rind, 1998; O'Brien & Currie, 1993). External forcing at the interdecadal scale is extremely weak, yet 20-year cycles are common in many time series (Burroughs, 1992).
6. There appears to be an increase in the interannual variability around the time of the major interdecadal regime shifts.

5.2. Characteristics of chaotic systems

The attributes of the North Pacific that are outlined above describe a quasi-periodic structure with irregular behavior; these are also characteristics of low-order chaotic systems. Low-order chaotic systems are models of complex physical processes based on non-linear ordinary differential equations and a small number (N) of variables. The solution to the system of equations is sensitive to the coefficients of the nonlinear terms and the magnitude of the forcing terms. The solution for the set of equations at any given time exists as a location in an N-dimensional space, where each variable represents one dimension. This forms a Euclidean phase space. The time dependence of the solutions is called the trajectory in phase space. The trajectory can evolve toward a fixed point, increase without bound, approach a limit cycle where the solution has a periodic trajectory, or have a chaotic character. The evolution of the trajectory is sensitive to initial conditions. A trajectory may never return to exactly the same location, and nearby trajectories often diverge. Systems with broad-banded time-frequency spectra will often have a non-periodic trajectory, but one that will be confined to a finite volume of the phase space, called the attractor. Even though a chaotic system can be defined by simple deterministic rules, its energy spectrum is similar to one created through statistical random processes. However, an important difference between mathematical chaos and random processes is that the statistical model will span the geometric N-dimensional space, while mathematical chaos will have an attractor of limited volume. Theoretically, one can know more about the chaotic system than can be described from a strictly random process.

Lorenz (1963) presented an example of a forced/damped chaotic system. His system of three equations was based on a convective model, but the tendency for the system's trajectory to lie near two locations in phase space, called fixed points, has made it a common analog for weather and climate comparisons (Palmer, 1993). The time series of the variable representing intensity of overturning from the Lorenz model shows two time scales, a rapid oscillation and slower time scale when the system can switch between two regimes with different convective intensities (Fig. 9).

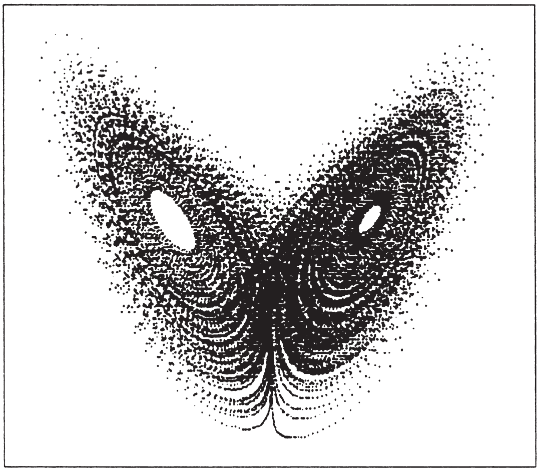

Fig. 9. The solution trajectory for the Lorenz (1963) model plotted in two dimensions. The solution never repeats itself exactly, but tends to stay in the vicinity of either of the fixed points or transitions from one fixed point to the other.

There are two relevant conclusions from the study of simple chaotic systems. The first is that, if the trajectory is near one of the fixed points, it will tend to stay near the fixed point or translate smoothly to the other fixed point. Small perturbations to the system will not change its trajectory significantly. However, if the system state is far from the two fixed points, its trajectory will be sensitive to small perturbations and will have large amplitude oscillations. Thus the stability of the system and its response to external forcing are time dependent. The second conclusion is that when the external forcing changes, the phase position of the two fixed points does not change, but there is a change in the probability of finding the state near the two fixed points (Palmer, 1999).

Another relevant chaos model is the "simplest possible general circulation model (GCM)" of Lorenz (1990). The primary variable represents the strength of a large-scale west wind or the geostrophically equivalent large-scale north/south atmospheric temperature gradient. The second and third variables are the strengths of the cosine and sine phases of a chain of superposed waves. The time scale for this system is days, and it is forced by a north/south temperature gradient and an east/west asymmetry. When the forcing is constant, the solution shows no pronounced variation with periods of a year or longer. However, when a seasonal cycle is added by allowing the north/south temperature gradient to vary over a year, decadal time-scale variations in the model's climate are generated that are on the same order as interannual variations (Pielke & Zeng, 1994). No long-term physical mechanisms are required to account for the substantial long-term deviations. This type of forced/damped system generates energy in periods that are multiples of each other. Through doubling, the Lorenz simple GCM shows that decadal scale variability can be generated from a high-frequency model of daily weather when its forcing is varied through an annual cycle. The importance of seasonality on interannual variability of winter dynamics in the

North Pacific was noted by Newman and Sardeshmukh (1998). Jin, Neelin and Ghil (1994) noted the importance of the annual cycle on the ENSO system.

Simple ocean box models can be added to the Lorenz simple GCM to represent the coupled atmosphere/ocean system. High-frequency atmospheric forcing drives an ocean whose response feeds back low-frequency changes to the atmospheric boundary conditions. Zondervan (1996) developed this kind of coupled model. Fig. 10 shows an example of his results with the upper time series showing the strength of the zonal wind, and lower time series showing the ocean temperature. The relationship between high-frequency and low-frequency variance in the two time series begs a comparison between the interannual and multi-decadal energy in the NPI and the PDO.

5.3. A chaotic conceptual model for the North Pacific

The similarities between the North Pacific and chaotic systems outlined above imply that a new conceptual model can be considered for the North Pacific whereby it is described as a forced dissipative system organized by underlying dynamic principles. This organization is achieved by air/sea interaction processes that suggest decadal scale coupling (Münnich, Latif, Venzke & Maier-Reimer, 1998; Neelin & Wang, 1999). It is straightforward to start with a system of non-linear equations and

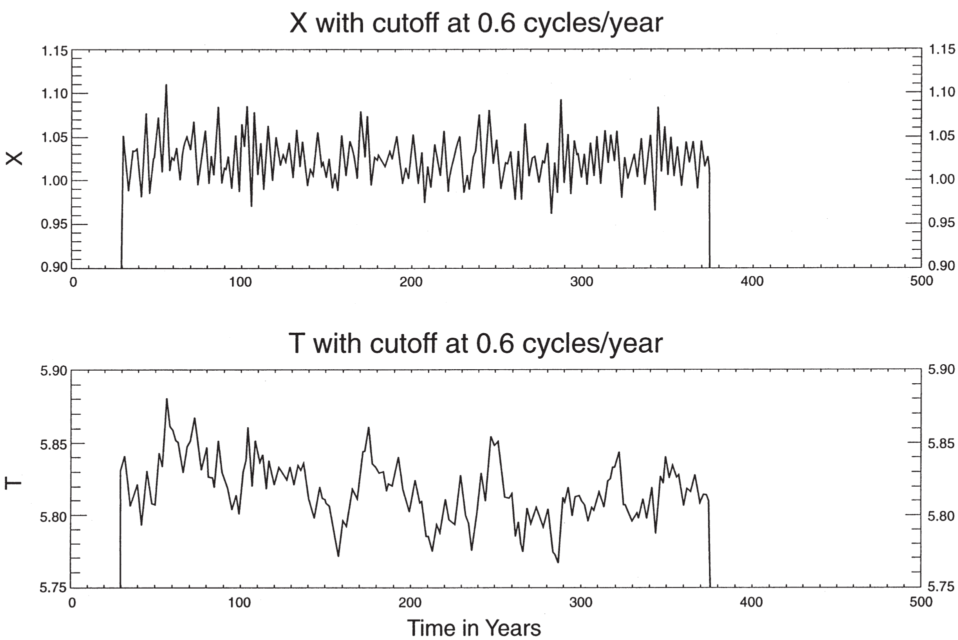

Fig. 10. The results of a simple atmosphere/SST chaos model (Zondervan, 1996). Top panel shows the strength of the zonal wind (X); bottom panel shows the SST (T) in a forced response ocean. The relationship between high- and low-frequency variability in these figures has the same character as the NPI and the PDO.

describe the outcomes, but it is much more difficult to start with the observational record and deduce the underlying system. The observational time series are too short to rigorously show the presence of chaotic dynamic processes (Cambel, 1993). What we can say is that the North Pacific shows several properties that subjectively fit a chaotic model, rather than an oscillator or statistical steady-state model. The North Pacific system may not be fully chaotic, but it shows intermittent nonlinear behavior (Zimmer, 1999).

Although the Northern Hemisphere climate undergoes continual fluctuations, it does have a tendency to linger in preferred states or fixed points, characterized by explicit large-scale spatial patterns (Kimoto & Ghil, 1993; Corti, Molteni & Palmer, 1999; Smyth, Ide & Ghil, 1999). Corti et al. (1999) used a reduced set of 500 mb geopotential heights from 1949–94 to show that the probability density function of the state space had four maxima, none of which was Gaussian around the origin. Two of the maxima have projections on the Pacific North American (PNA) pattern. The PNA is a well-known tropospheric pattern based on 500 mb flow which is more zonal in its negative phase and has greater north–south amplitude in its positive phase (Rossby et al., 1939; Wallace, Zhang & Lau, 1993; Lin & Derome, 1997). The PNA is also shown to be coupled to the PDO (Wallace, Smith & Bretherton, 1992). The positive and negative phases of the PNA play an important part in the preferred cycles of northern hemispheric variability (Molteni, Tibaldi & Palmer, 1990; Haines & Hannachi, 1995). The North Pacific appears to have a few preferred states, but no state is an exact repeat.

The preferred states of the North Pacific ocean–atmosphere system tend to be stable, meaning the system is less responsive to changes in the external forcing. But there are other states, i.e. locations in the phase space, where small external changes can force rapid transitions to the other states. Examples of external forcing parameters might be SST anomalies, El Niño/La Niña, sea ice extent, snow cover, or solar or lunar phases. Climate shifts in the North Pacific on decadal and longer timescales may be triggered by extreme events in a given year. For example, Watanabe and Nitta (1999) suggest the 1989 shift in the Aleutian low was related to extreme Siberian snow cover. Wooster and Hollowed (1995) noted that warm eras in the northeast Pacific could be initiated by ENSO. Further examination of Fig. 3, which contains our PC1 and PC2 time series representing the PDO and Niño North respectively, shows that many of the large shifts in the PDO (1958, 1962, 1989) were preceded by strong Niño North events (1957, 1961, and 1988). However, not all decadal North Pacific SST shifts are associated with ENSO events. For example, the 1977 shift was preceded by a year with record ice extent in the Bering Sea. In this example, the PDO and Niño North could be considered a 2-dimensional phase space for the North Pacific.

The presence of La Niña conditions in 1998–1999, the extremely large positive spike in the Niño North time series (Fig. 3) for 1999, and the recent extreme variability of sea ice in the Bering Sea may be indicators of a shift in the PDO for 1999. Hare and Mantua (2000) note that SSTs along the Pacific coast of North America have been cooler than normal since late 1998, and they also suggest that the PDO may have shifted to its negative phase. Large recent interannual variability would be consistent with this type of system transition.

6. Summary

The energy content of North Pacific time series are broad banded and temporally irregular. The PDO has relatively more interdecadal and pentadecadal energy than the NPI or the Sitka air temperature (Table 1). This may result from either ocean coupling or the predominance of the central Pacific SST contribution to the PDO. The decadal variability in NPI and Sitka air temperature shifted smoothly from about 8 to 20 years during the 20th century. A chaotic conceptual model has been applied to the North Pacific that is consistent with the observed irregular behavior and suggests that the transitions from one state to another are rapid rather than gradual. It should be noted, however, that the time series are too short to prove that the North Pacific is chaotic.

Should we be disappointed that the North Pacific exhibits chaotic behavior? The disappointment might come from the more general definition of chaos which is "any great confusion or disorder." But the use of the word chaos in the context of this paper implies that there is order behind the irregularity of the system. A chaotic trajectory tends to return to the vicinity of its previous location, and there are only a few quasi-stable states. This return occurs more often than would be expected statistically, given the observed variance of the time series (Tsonis, 1992). There is evidence that the PNA behaves like a fixed point of a chaotic attractor (Hannachi, 1997) and that it is coupled to the PDO (Wallace et al., 1992). The feedback between the atmosphere and the ocean promotes decadal signals. Careful averaging also can lower the dimensions of the system and make it more amenable to analysis (Nicolis & Nicolis, 1995).

A chaotic conceptual model may lead to better understanding of the low-frequency relationship between physical and biological systems in the North Pacific. One characteristic of a chaotic system is that near the time of major interdecadal transition there would be several years of extreme, and perhaps opposite, anomalies in the physical system. These extreme anomalies provide opportunities for change in the biological system. The late 1990s may provide an example of this type of transitional period.

Acknowledgements

This manuscript is a contribution to the Fisheries Oceanography Coordinated Investigations (FOCI). We thank the reviewers for suggesting important clarifications. We gratefully acknowledge the support of NASA Polar Programs and the North Pacific Marine Research Initiative (NPMR). This publication was supported by the Joint Institute for the Study of the Atmosphere and Ocean (JISAO) under NOAA Cooperative Agreement #NA67RJO155, Contribution #757. PMEL Contribution #2068.

References

Burroughs, W. J. (1992). *Weather cycles: real or imaginary*? Cambridge University Press. 201 pp.

Cambel, A. B. (1993). *Applied chaos theory: a paradigm for complexity*. San Diego, CA: Academic Press. 246 pp.

Corti, S., Molteni, F., & Palmer, T. N. (1999). Signature of recent climate change in frequencies of natural atmospheric circulation. *Nature, London*, *398*, 799–802.

Daubechies, I. (1994). Ten lectures on wavelets CBMS. *SIAM*, *61*, 194–202.

Davis, R. E. (1976). Predictability of sea surface temperature and sea level pressure anomalies over the North Pacific Ocean. *Journal of Physical Oceanography*, *6*, 249–266.

Hannachi, A. (1997). Low frequency variability in a GCM: three-dimensional flow regimes and their dynamics. *Journal of Climate*, *10*, 1357–1379.

Haines, K., & Hannachi, A. (1995). Weather regimes in the Pacific from a GCM. *Journal of Atmospheric Science*, *52*, 2444–2462.

Hare, S. R., & Mantua, N. J. (2000). Empirical evidence for North Pacific regime shifts in 1977 and 1989. *Progress in Oceanography*, *47*, 103–145.

Hoerling, M. P., & Kumar, A. (1997). Why do North American climate anomalies differ from one El Niño event to another? *Geophysical Research Letters*, *99*, 1059–1062.

Hollowed, A. B., Hare, S. R., & Wooster, W. S. (1998). Pacific basin climate variability and patterns of northeast Pacific marine fish production. In *Proceedings, 'A ha Huliko'a Hawaiian Winter Workshop January 25–29, 1998* (pp. 89–104). (available from P. Muller, University of Hawaii, 1000 Pope Road, Honolulu, HI 96822).

Iwasaka, N., Hanawa, K., & Toba, Y. (1988). Partition of the North Pacific Ocean based on similarity in temporal variations of the SST anomaly. *Journal of the Meteorological Society of Japan*, *66*, 433–443.

Jin, F., Neelin, J. D., & Ghil, M. (1994). El Niño on the Devil's staircase: annual subharmonic steps to chaos. *Science*, *264*, 70–72.

Kimoto, M., & Ghil, M. (1993). Multiple flow regimes in the Northern Hemisphere winter. Part I: methodology and hemispheric regions. *Journal of the Atmospheric Sciences*, *50*, 2625–2643.

Lagerloef, G. S. E. (1995). Interdecadal variations in the Alaskan gyre. *Journal of Physical Oceanography*, *25*, 2242–2258.

Lau, K. M., & Weng, H. (1995). Climate signal detection using wavelet transform: how to make a time series sing. *Bulletin of the American Meteorological Society*, *76*, 2391–2402.

Lean, J., & Rind, D. (1998). Climate forcing by changing solar radiation. *Journal of Climate*, *11*, 3069–3094.

Leathers, D. J., & Palecki, M. A. (1992). The Pacific/North American teleconnection pattern and United States climate. Part II: temporal characteristics and index specification. *Journal of Climate*, *5*, 707–716.

Lin, H., & Derome, J. (1997). On the modification of high- and low-frequency eddies associated with the PNA anomaly: an observational study. *Tellus*, *49A*, 87–99.

Lorenz, E. N. (1963). Deterministic nonperiodic flow. *Journal of Atmospheric Science*, *20*, 130–141.

Lorenz, E. N. (1990). Can chaos and intransitivity lead to interannual variability? *Tellus*, *42A*, 378–389.

Mantua, N. J., Hare, S. R., Zhang, Y., Wallace, J. M., & Francis, R. C. (1997). A Pacific interdecadal climate oscillation with impacts on salmon production. *Bulletin of the American Meteorological Society*, *78*, 1069–1079.

Minobe, S. (1999). Resonance in bidecadal and pendecadal climate oscillation over the North Pacific: role in climate regime shifts. *Geophysical Research Letters*, *26*, 855–858.

Molteni, F., Tibaldi, S., & Palmer, T. N. (1990). Regimes in the wintertime circulation over northern extratropics. I: observational evidence. *Quarterly Journal of the Royal Meteorological Society*, *116*, 31–67.

Münnich, M., Latif, M., Venzke, S., & Maier-Reimer, E. (1998). Decadal oscillations in a simple coupled system. *Journal of Climate*, *11*, 3309–3319.

Neelin, J. D., & Wang, W. (1999). Analytical prototypes for ocean–atmosphere interaction at midlatitudes. Part I: coupled feedbacks as a sea surface temperature dependent stochastic process. *Journal of Climate*, *12*, 697–721.

Newman, M., & Sardeshmukh, P. D. (1998). The impact of the annual cycle on the North Pacific/North

America response to remote low-frequency forcing. *Journal of the Atmospheric Sciences*, *55*, 1336–1353.

Nicolis, C., & Nicolis, G. (1995). From short-scale atmospheric variability to global climate dynamics: toward a systematic theory of averaging. *Journal of the Atmospheric Sciences*, *52*, 1903–1913.

O'Brien, D. P., & Currie, R. G. (1993). Observations of the 18.6-year cycle of air pressure and a theoretical model to explain certain aspects of this signal. *Climate Dynamics*, *8*, 287–298.

Overland, J. E., Adams, J. M., & Bond, N. A. (1999). Decadal variability of the Aleutian low and its relation to high latitude circulation. *Journal of Climate*, *12*, 1542–1551.

Palmer, T. N. (1993). Extended-range atmospheric prediction and the Lorenz Model. *Bulletin of the American Meteorological Society*, *74*, 49–65.

Palmer, T. N. (1999). A nonlinear dynamical perspective on climate prediction. *Journal of Climate*, *12*, 575–591.

Parker, D. E., Folland, C. K., & Jackson, M. (1995). Marine surface temperature: observed variations and data requirements. *Climatic Change*, *31*, 559–600.

Percival, D. B., & Mofjeld, H. O. (1997). Analysis of subtidal coastal sea levels using wavelets. *Journal of the American Statistical Association*, *92*, 868–880.

Pielke, R. A., & Zeng, X. (1994). Long-term variability of climate. *Journal of the Atmospheric Sciences*, *51*, 155–159.

Rossby, C.-G. and co-authors (1939). Relation between variations in the intensity of the zonal circulation in the atmosphere and displacements of the semi-permanent centers of action. *Tellus*, 2, 275–301.

Royer, T. C. (1989). Upper ocean temperature variability in the northeast Pacific: is it an indicator of global warming? *Journal of Geophysical Research*, *94*, 18175–18183.

Royer, T. C. (1993). High-latitude oceanic variability associated with the 18.6-year nodal tide. *Journal of Geophysical Research*, *98*, 4639–4644.

Salmon, D. K. (1992). *On interannual variability and climate change in the North Pacific*, Ph.D. thesis. University of Alaska, Fairbanks. 219 pp.

Seckel, G. R. (1993). Zonal gradient of the winter sea level atmospheric pressure at 50°N: an indicator of atmospheric forcing of North Pacific surface conditions. *Journal of Geophysical Research*, *98*, 22615–22628.

Smyth, P., Ide, K., & Ghil, M. (1999). Multiple regimes in Northern Hemisphere height fields via mixture model clustering. *Journal of the Atmospheric Sciences*, *56*, 3704–3723.

Tanaka, H. L., Kanohgi, R., & Yasunari, T. (1996). Recent abrupt intensification of the northern polar vortex since 1988. *Journal of the Meteorological Society of Japan*, *74*, 947–954.

Torrence, C., & Campo, G. P. (1998). A practical guide to wavelet analysis. *Bulletin of the American Meteorological Society*, *79*, 61–78.

Trenberth, K. E., & Hurrell, J. W. (1994). Decadal atmosphere–ocean variations in the Pacific. *Climate Dynamics*, *9*, 303–319.

Tsonis, A. A. (1992). *Chaos: from theory to applications*. New York: Plenum Press. 274 pp.

Wallace, J. M., Smith, C., & Bretherton, C. S. (1992). Singular value decomposition of wintertime sea surface temperature and 500-mb height anomalies. *Journal of Climate*, *5*, 561–576.

Wallace, J. M., Zhang, Y., & Lau, K. (1993). Structure and seasonality of interannual and interdecadal variability of the geopotential height and temperature fields in the Northern Hemisphere troposphere. *Journal of Climate*, *6*, 2063–2082.

Watanabe, M., & Nitta, T. (1999). Decadal changes in the atmospheric circulation and associated surface climate variations in the northern hemisphere winter. *Journal of Climate*, *12*, 494–510.

Wooster, W. S., & Hollowed, A. B. (1995). Decadal-scale variations in the eastern subarctic Pacific: I. Winter ocean conditions. In R. J. Beamish (Ed.), *Climate change and northern fish populations* (pp. 81–85), Canadian Special Publication of Fisheries and Aquatic Sciences, 121, National Research Council of Canada, Ottawa.

Zimmer, C. (1999). Life after chaos. *Science*, *284*, 83–86.

Zondervan, G. (1996). Chaos and coupling: A coupled atmosphere ocean-box model for coupled behaviour studies. *Wetenschappelijk Report (Koninklijk Nederlands Meteorologisch Instituut)*, WR 96-02. 41 pp.